doi: 10.15407/ujpe62.04.0285

V.O. ZHELTONOZHSKYI,[1] A.M. SAVRASOV,[1] K.M. SOLODOVNYK,[1,2]
V.A. PLUJKO,[2] O.M. GORBACHENKO,[2] O.I. DAVYDOVSKA[1]

[1] Institute for Nuclear Research, Nat. Acad. of Sci. of Ukraine
(47, Nauky Ave., Kyiv 03028, Ukraine; e-mail: zhelton@kinr.kiev.ua)
[2] Taras Shevchenko National University of Kyiv, Faculty of Physics
(60, Volodymyrs'ka Str., Kyiv 01033, Ukraine)

ISOMER RATIOS AND MEAN ANGULAR MOMENTA OF PRIMARY ^{97}Nb FRAGMENTS AT ^{235}U AND ^{238}U PHOTOFISSION

PACS 25.85.Jg

The isomeric yield ratios are measured for ^{97}Nb fragments obtained at the bremsstrahlung photofission of ^{235}U and ^{238}U nuclei with gamma-quantum end-point energies of 10.5, 12.0, and 18.0 MeV. The mean angular momenta of primary fission fragments are determined, by using the generalized Huizenga–Vandenbosh statistical model and with the help of TALYS 1.6 and EMPIRE 3.2 codes.

Keywords: photofission, isomeric ratios, mean angular momenta of fission fragments.

1. Introduction

Processes of nuclear fission have been studied for a long time. However, some issues concerning their dynamics remain unresolved till now. While studying variations of nuclear properties at the transition from the saddle point to the scission one, the determination of the angular momenta of fission fragments is very important. For example, in the framework of the droplet nuclear model, the emergence of high angular momenta is explained by the excitation of modes associated with the rotation of fission fragments. In particular, the increase of angular momenta in comparison with that of the parent compound nucleus may testify to the presence of mechanisms that spin up the fragments owing to the action of Coulomb and nuclear forces after the fissioning nucleus breaks up [1–4]. One of the methods for the determination of the angular momenta of fission fragments is the method of isomeric ratios.

Conventionally, the isomeric ratio R_σ is the ratio between the cross-section of the reaction with the population of a metastable state to the cross-section of the reaction with the population of the ground state: $R_\sigma = \sigma_m/\sigma_g$. But $R_\sigma = \sigma_g/\sigma_m$ is adopted, as a rule, if $J_m < J_g$. In photonuclear reactions under the influence of bremsstrahlung gamma quanta with the energy ranging from the reaction threshold to the end energy E_e, the isomeric yield ratio is measured as the ratio between the reaction yields with the formation of a metastable state and the ground one: $R_Y = Y_m/Y_g$ or $R_Y = Y_g/Y_m$. Note that, according to Refs. [5, 6], the isomeric ratios R_σ and R_Y practically coincide for photonuclear reactions with the energy $E_e \leq 20$ MeV.

This work continues a cycle of researches dealing with the isomeric ratios and the mean angular momenta of photofission fragments of actinide nuclei (see Refs. [7–11] and references therein). Its aim consists in the determination of the isomeric yield ratios for the primary ^{97}Nb nucleus fragment and the determination of its mean angular momentum in the photofission reactions of ^{238}U and ^{235}U nuclei with

the use of the bremsstrahlung with various end-point energies.

2. Experimental Part. Measurement Technique

For the determination of the reaction yields, the activation technique was used. Spectrometric measurements allow the induced activity of researched isotopes to be determined from characteristic peaks in the gamma spectrum registered at a definite time moment. If the isomeric ratios are dealt with, the areas under the peaks of the total absorption corresponding to the γ-transition of a nucleus from the isomeric to the ground state and the γ-transition at the decay of the ground state of a nucleus, which is unstable for ^{97}Nb, are determined and compared with each other. In photofission reactions, besides the direct population of the nucleus in the isomeric state, isotopes from the parent isobaric chain are also formed. As a result of the β-decay, such isobaric nuclei can give a considerable contribution to the nuclear population in addition to the direct population at the fission. This contribution of isobaric nuclei should be taken into account, because the direct population can be several times lower. For this purpose, the area under the peak of total absorption arising due to the decay of a precursor nucleus is determined additionally. The schematic diagram of the analyzed chain of decays is depicted in Fig. 1.

The time evolution of the numbers of nuclei that are formed in the ground, N_g, and metastable, N_m, states, as well as the isobaric nuclei, N_b, is described

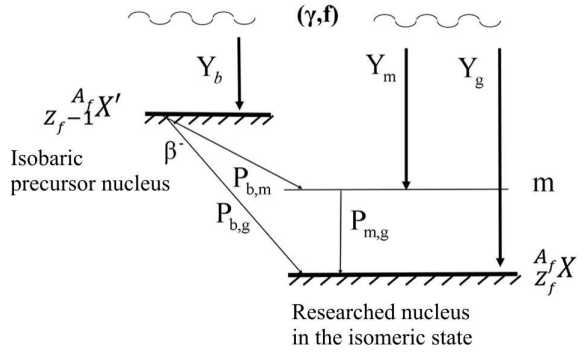

Fig. 1. Schematic diagram for the population of the ground and isomeric states of the $^{A_f}_{Z_f}X$ nucleus at the parent nucleus fission. The contribution to the population from the isobaric precursor nucleus $^{A_f}_{Z_f-1}X'$ is taken into account

by the following system of kinetic equations:

$$\begin{cases} \dfrac{dN_b(t)}{dt} = Y_b\Theta\left(t_{\rm ir}-t\right) - \lambda_b N_b\left(t\right), \\ \dfrac{dN_m(t)}{dt} = Y_m\Theta\left(t_{\rm ir}-t\right) + P_{b,m}\lambda_b N_b\left(t\right) - \\ -\lambda_m N_m\left(t\right), \\ \dfrac{dN_g(t)}{dt} = Y_g\Theta\left(t_{\rm ir}-t\right) + P_{m,g}\lambda_m N_m\left(t\right) + \\ +P_{b,g}\lambda_b N_b\left(t\right) - \lambda_g N_g\left(t\right), \end{cases} \tag{1}$$

where the subscripts m and g designate the metastable and ground, respectively, states of the studied nucleus; the subscript b means the isobaric precursor nucleus; N_m, N_g, and N_b are the numbers of nuclei in the corresponding states; λ_m, λ_g, and λ_b are the constants of nuclear decay; Y_m, Y_g, and Y_b are the yields of reactions with the formation of nuclei in the metastable and ground states, and the precursor nuclei from the corresponding β-decay chain; $P_{b,g}$ and $P_{b,m}$ are the fractions of isobaric nuclei that populate the ground and metastable, respectively, states at the decay; and $P_{m,g}$ is the fraction of nuclei decaying from the metastable state into the ground one. This system describes the processes of straightforward generation of the element during the nuclear reaction, its formation owing to the decay of the precursor nucleus, and the reduction of the number of nuclei as a result of their radioactive decay.

In the course of spectrometric experiments carried out following the activation technique, the specimen was first irradiated within the time interval $t_{\rm ir}$. Then it was cooled down and transported to a spectrometer during the time interval $t_{\rm col}$. At last, the number of counts was measured within the time interval t_m. This number is related with the areas under the photo-peak S_i ($i = m,\ g,\ b$) and with the number of nuclei $N_i(t)$ by the formula

$$S_i(t_m) = f_i\,\varepsilon_i\,\lambda_i \int\limits_{t_0}^{t_1} N_i(t)\,dt,$$

where f_i is the emission probability for the given gamma quantum, ε_i the efficiency of registration by a spectrometer at the given energy, $t_0 = t_{\rm ir} + t_{\rm col}$, and $t_1 = t_{\rm ir} + t_{\rm col} + t_m$.

The isomeric ratios R_Y were calculated as the ratio Y_g/Y_m between the reaction yields that satisfied Eqs. (1) provided the fixed experimental values of areas S_i ($i = m, g, b$) under the total absorption

peaks. The calculations were carried out with the help of the software code IZOMER [8].

Specimens were irradiated on an M-30 microtron (Institute of Electron Physics of the National Academy of Sciences of Ukraine, Uzhgorod), by using γ-quanta of the electron bremsstrahlung spectrum. A thin tantalum plate was used as a bremsstrahlung target. Therefore, the bremsstrahlung spectrum looked like the Schiff one. The maximum energy of bremsstrahlung gamma quanta, E_e, was 10.5, 12.0, and 18.0 MeV.

A closed ^{235}U source (90% ^{235}U + 10% ^{238}U, 514 mg in mass, and packed into a container) and a ^{238}U specimen (stripes from evaporated ^{238}U with a total isotope mass of 2 g) were used as targets. Figure 2 schematically illustrates the geometry of the irradiated ^{238}U specimen. The surface of aluminum foils was a place, where radioactive fragments that were emitted at the uranium fission were deposited. After the irradiation, the gamma spectra of fission fragments in the activated foils were analyzed on a spectrometer.

The gamma spectra of activated targets were measured on a spectrometer equipped with an HPGe detector. The spectrometer resolution was equal to 2.0 keV at the γ-transition with $E_\gamma = 1332.5$ keV in ^{60}Co nucleus. The spectra were registered every 60 s during the whole measurement time interval t_m. The data obtained for the end-point irradiation energies of the uranium specimen, the irradiation time interval $t_{\rm ir}$, the total time of cooling and transportation $t_{\rm col}$, and the maximum total time of measurements are quoted in Table 1. An example of the obtained photofission spectra is depicted in Fig. 3.

Table 1. **End-point energies of uranium specimen irradiation, irradiation times, cooling times, and total times of spectrum measurement**

Target nucleus	^{235}U		^{238}U	
	Exp. 1	Exp. 2	Exp. 3	Exp. 4
End-point energy of γ quanta (MeV)	10.5	18.0	12.0	18.0
Irradiation time $t_{\rm ir}$ (min)	10.0	5.0	20.0	10.0
Total time of cooling and transportation $t_{\rm col}$ (s)	28.0	166.0	49.0	37.0
Total time of spectrum measurement $t_{\rm mes}$ (min)	858.0	46.0	309.0	1083.0

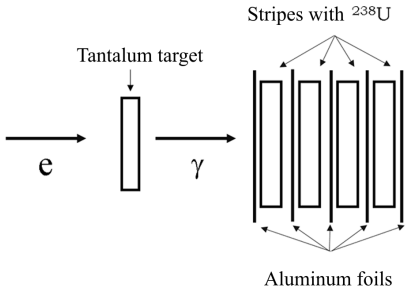

Fig. 2. Experimental setup for the irradiation of specimens with ^{238}U

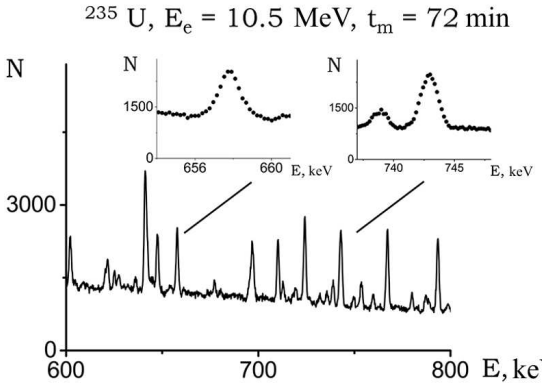

Fig. 3. Fragment of the characteristic ^{235}U photofission spectrum, which was used for the calculation of isomeric ratios. The scaled-up sections of the spectrum detail the spectral intervals containing the peaks from gamma transitions with $E_\gamma = 658.13$ and 743.36 keV. The corresponding end-point irradiation energy and measurement time are indicated in the figure, E is the energy registered by a gamma detector, and N the total number of counts within the time interval t_m

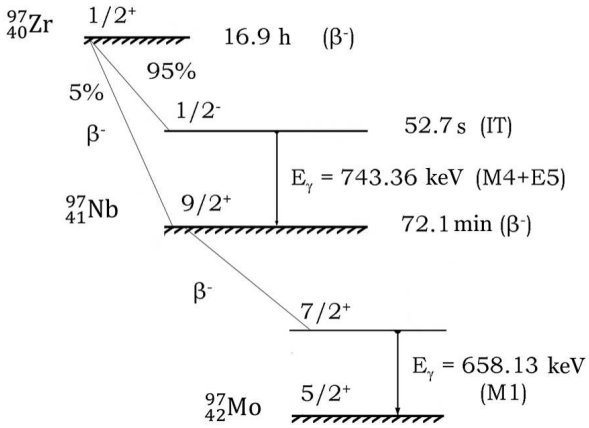

Fig. 4. Fragment of the fission chain ^{97}Zr $\rightarrow$ ^{97}Nb $\rightarrow$ ^{97}Mo. Transitions with $E_\gamma = 743.36$ and 658.13 keV were used to determine the level populations. The parameters of states and transitions are taken from Ref. [13]

The photofission spectra were used to calculate the isomeric ratios for ^{97}Nb with regard for the contribution from the isobaric nucleus ^{97}Zr. A fragment of the decay scheme $^{97}\text{Zr} \rightarrow {}^{97}\text{Nb} \rightarrow {}^{97}\text{Mo}$ is shown in Fig. 4.

The registered gamma spectra were analyzed with the use of the Winspectrum software package [12]. The calculations were rather complicated, because 1) there was a necessity to measure the spectra during different time intervals, which corresponded to the half-life periods of the examined isotope states, with the subsequent normalization of the N_m-, N_g-, and N_b-values calculated from those spectra to a certain identical measurement time interval t_m; 2) the peaks of total absorption considerably overlapped one another; and 3) the influence of the dead time during the first minutes of measurements was significant (10–80%).

When calculating the populations, the most intense gamma transitions in the decay chain $^{97}\text{Zr} \rightarrow {}^{97}\text{Nb} \rightarrow$ $\rightarrow {}^{97}$Mo were used. Namely,

• the population N_b of the ground state of the isobaric precursor nucleus ^{97}Zr was determined from the area under the gamma-transition peak with $E_\gamma =$ $= 743.36$ keV associated with the decay $^{97}\text{Zr} \rightarrow$ $\rightarrow {}^{97m}\text{Nb}$ ($T_{1/2} = 16.9$ h);

• the population N_m of the metastable state ^{97m}Nb was determined from the area under the gamma-transition peak with $E_\gamma = 743.36$ keV associated with the decay $^{97m}\text{Nb} \rightarrow {}^{97g}\text{Nb}$ ($T_{1/2} = 52.7$ s);

• the population N_g of the ground state of ^{97g}Nb was determined from the area under the gamma-transition peak into the second excited state with $E_\gamma = 658.13$ keV associated with the decay $^{97g}\text{Nb} \rightarrow$ $\rightarrow {}^{97}$Mo ($T_{1/2}$ =72.1 min).

Owing to a substantial difference between the half-life periods of the examined isotopes, the calculation of contributions of all gamma transitions from the same spectrum corresponding to a certain chosen measurement time t_m would be characterized by a low statistical accuracy. For this reason, in order to calculate the number of generated nuclei correctly, the areas under the peaks were calculated for the spectra registered at the times, when the contributions from the examined isotopes were maximum. Afterward, the areas under the peaks were recalculated to the same time interval t_m. The time t_m for each experiment was selected to be close as much as possible to the half-life period of the decay $^{97g}\text{Nb} \rightarrow {}^{97}$Mo. The areas under the peaks were determined as follows.

• The area S_b under the peak with $E_\gamma = 743.36$ keV for ^{97}Zr nucleus with $T_{1/2} = 16.9$ h was calculated from the difference between the spectra measured during the $\left(t = 10T_{1/2}\right)$- and $\left(t = T_{1/2}\right)$-time intervals (i.e. from the difference between the spectra measured during 1010 and 10 min). If the measurement lasted less than 16.9 h, conditions close to the indicated ones as much as possible were used.

• Since the loss of counts during the dead time had to be taken into account for the short-lived ^{97m}Nb, the areas under the peak with $E_\gamma = 743.36$ keV were separately determined at the first and second minutes of the measurement. Then the calculated contribution S_b was subtracted, and a correction for the dead time was made.

• The area S_g under the peak was determined directly from the spectrum corresponding to the measurement time t_m.

In addition, if it was possible, the areas $S_{m,g,b}$ for the indicated gamma transitions were determined from the spectra measured during $t = T_{1/2}$, $2T_{1/2}$, ..., and so on in order to test the time variations of the areas under the peaks, which should correspond to the radioactive decay law.

When determining the areas S_b, S_m, and S_g, the spectra processing was performed making allowance for the contributions inserted by external elements, i.e. by other photofission products, the gamma transitions of which have energies close to the considered values, which were not resolved by a spectrometer and created the overlapping. Such contributions were determined with regard for the intensity ratio for the gamma transitions of the foreign isotope. The correspondence of the time evolution of the areas under the peaks of total absorption to the radioactive decay law of the analyzed foreign element was additionally verified. The calculation of the peak areas for elements with long lifetimes was carried out from the difference between the spectra corresponding to ten half-life periods of all short-lived elements and the spectra corresponding to one half-life period of the long-lived element after the decay of short-lived ones. The decay chains of foreign elements, their half-life periods, and the energies of γ-transitions, which were used to determine their contributions, are quoted in Table 2.

The complicated configuration of the target with ^{235}U made it impossible to perform the external effi-

Table 2. **Nuclear fission chains, their half-life times, and lines used when processing the spectrum in order to determine the area under the peaks S_b, S_m, and S_g**

Fission chains	$^{134}\mathrm{Te}\to$ $\to{}^{134}\mathrm{I}$	$^{130}\mathrm{Sn}\to$ $\to{}^{130}\mathrm{Sb}$	$^{128m}\mathrm{Sb}\to$ $\to{}^{128}\mathrm{Te}$	$^{128g}\mathrm{Sb}\to$ $\to{}^{128}\mathrm{Te}$	$^{128}\mathrm{Sn}\to{}^{128m}\mathrm{Sb}\to$ $\to{}^{128}\mathrm{Te}$	$^{89}\mathrm{Rb}\to$ $\to{}^{89}\mathrm{Sr}$
Half-lifes (min)	41.8	3.7	10.4	540.6	59.1	15.2
Energy of transition that creates overlapping	742.6	743.1	743.2	743.2	743.2	657.8
Energy of transition used to calculate the contribution	566.0	779.8	753.9	753.9	753.9	1248.1

Table 3. **Results of calculation of the isomeric yield ratios for the ^{97}Nb fission fragment in ^{235}U and ^{238}U photofission reactions from experimental data**

Target nucleus	E_e, MeV	$R_Y = Y_g/Y_m$
^{235}U	10.5	0.75 ± 0.09
^{238}U	12.0	0.73 ± 0.10
^{235}U	18.0	3.9 ± 0.8
^{238}U	18.0	3.8 ± 0.6

ciency calibration. Therefore, in order to apply the same approach when processing the spectra of all specimens, a relative efficiency calibration was carried out for all four experiments, by using the measured gamma spectra of fission products. The registration efficiency of a spectrometer was calibrated on the basis of 35, on average, gamma transitions in fission fragments (^{146}Ce, ^{131}Te, ^{149}Nd, ^{101}Mo,^{134}I, ^{135}I, and ^{141}B), as well as using x-ray lines produced by uranium and lead. The efficiency curve was plotted, by following the method described in Ref. [12]. The obtained curves of the relative efficiency of gamma-radiation registration are exhibited in Fig. 5.

After determining the areas, Eqs. (1) were numerically solved with the help of the IZOMER code. The isomeric ratios were calculated as the yield ratios between the reaction into the state with the higher spin and the reaction into the state with the lower spin, $R_Y = Y_g/Y_m$. The resulting isomeric ratios obtained for ^{97}Nb are quoted in Table 3. The relevant measurement errors were evaluated as the statistical errors of the areas under the peaks of total absorption from the gamma transitions that correspond to the population of the ground and metastable states, and the decay of the isobaric precursor nucleus [9].

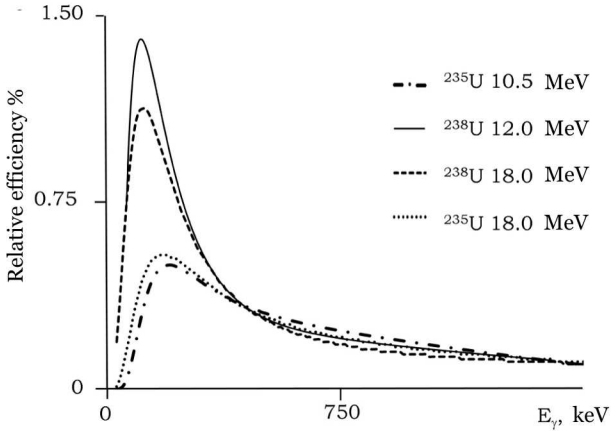

Fig. 5. Relative efficiency of the registration of gamma radiation for the photofission of ^{235}U and ^{238}U fragments under bremsstrahlung with various end-point energies

Note that the isomeric ratios for ^{95}Nb nucleus, the photofission fragment, were analyzed earlier in Ref. [7] in the cases of $^{232}\mathrm{Th}(n,f)$ reactions with a neutron energy of 14 MeV and $^{232}\mathrm{Th}(d,f)$ reactions with a deuteron energy of 13.6 MeV. The respective values of isomeric ratio $R_Y = Y_g/Y_m$ were found to equal 5.0 ± 1.0 and 3.6 ± 0.6. In Ref. [14], the isomeric yield ratios were measured for ^{97}Nb created in the reactions $^{98}\mathrm{Mo}(\gamma,\mathrm{p})^{97}\mathrm{Nb}$ and$^{100}\mathrm{Mo}(\gamma,\mathrm{p2n})^{97}\mathrm{Nb}$ with bremsstrahlung end-energies varying from 16.0 to 60.0 MeV. In particular, at $E_e = 16.0$ MeV, the isomeric yield ratio equals $R_Y = 1.740 \pm 0.141$. This fact testifies that the isomeric ratios can considerably depend on the type of the input channel.

3. Calculation of Mean Angular Momenta. Discussion of the Results Obtained

First, we should determine the spin distribution of initial states by fitting the values of isomeric ratios cal-

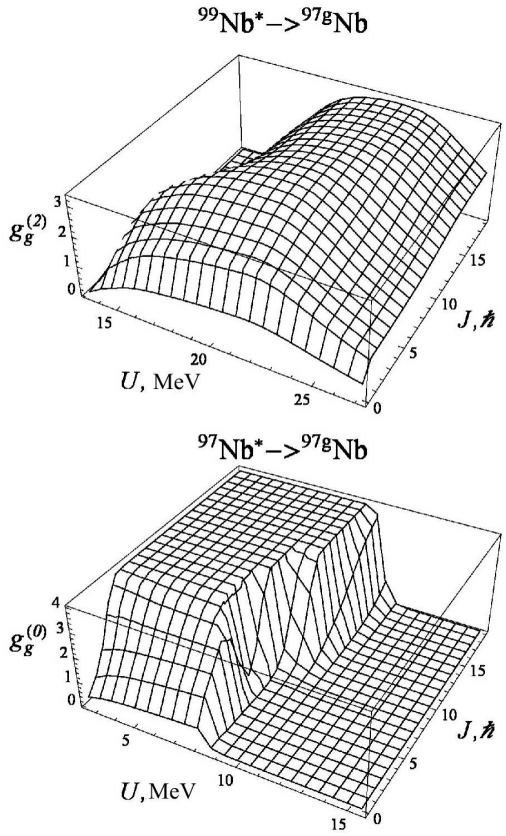

Fig. 6. Probabilities of the population of the ground state of ^{97}Nb nucleus from the states of excited isotopes ^{99}Nb and ^{97}Nb depending on the excitation energy U and the spin J, $g_g^{(i)}(U,J)$, calculated with the use of the EMPIRE 3.2 software code

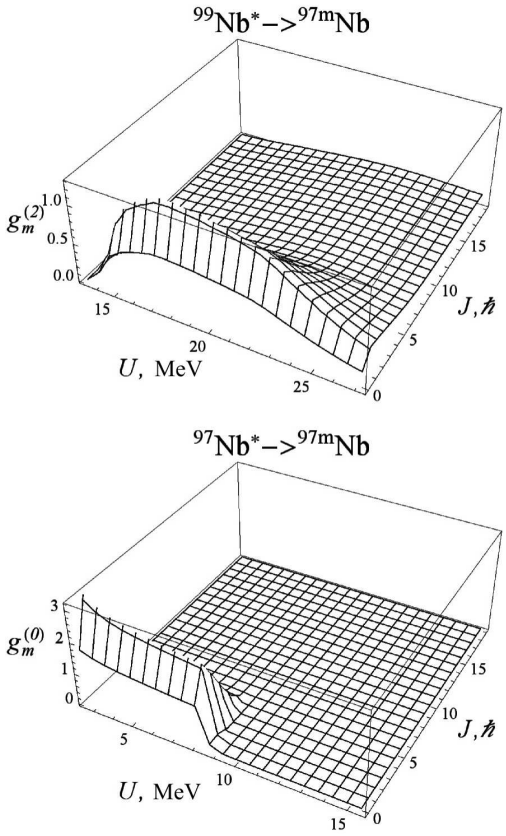

Fig. 7. Probabilities of population of the isomeric state of the ^{97}Nb nucleus from the states of excited isotopes ^{99}Nb and ^{97}Nb depending on the excitation energy U and the spin J, $g_m^{(i)}(U,J)$, calculated with the use of the EMPIRE 3.2 software code

culated theoretically to their experimental counterparts. When calculating the isomeric ratios, we used a generalization of the Huizenga–Vandenbosh statistical model, which was proposed in Refs. [9, 10]. Furthermore, we took into account the population of the ground (g) and metastable (m) states of the researched nucleus (A_f, Z_f) with charge Z_f emerging owing to the decay of isotopes $(A_i = A_f + i, Z_f)$ with a larger number of neutrons ($i \le i_m$). In particular, we made allowance for the contribution to the isomeric ratio produced by the decay of isotopes, in which the number of neutrons exceeded the number of neutrons in the nucleus (A_f, Z_f) by no more than two neutrons (the value $i_m = 2$ approximately corresponds to the average multiplicity of neutrons).

The populations $g_k^{(i)}(U,J)$ of the ground ($k = g$) and metastable ($k = m$) states of the nucleus (A_f, Z_f) that correspond to transitions with the emission of gamma quanta and neutrons from the nuclear states with the excitation energy U and the spin J were calculated with the use of the software codes EMPIRE 3.2 [16] and TALYS 1.6 [17].

For the calculation of isomeric ratios, the following expression was used:

$$R = \frac{\sum\limits_{i=0}^{i_m} \int\limits_{U_0^{(i)}}^{U_m^{(i)}} \sum\limits_J \Phi_i(A_i,U,J) \mathrm{g}_{\mathrm{g}}^{(i)}(U,J)dU}{\sum\limits_{i=0}^{i_m} \int\limits_{U_0^{(i)}}^{U_m^{(i)}} \sum\limits_J \Phi_i(A_i,U,J) \mathrm{g}_m^{(i)}(U,J)dU}, \qquad (2)$$

where

$$\Phi_i(A_i;U,J) = P(A_i)\varphi_i(U)P^{(i)}(J),$$

Table 4. **Results of theoretical calculations of the mean angular momenta**

Target nucleus (E_e, MeV)	TALYS				EMPIRE			
	$i_m = 0$		$i_m = 2$		$i_m = 0$		$i_m = 2$	
	Eq. (3)	Eq. (4)	Eq. (3)	Eq. (4)	Eq. (3)	Eq. (4)	Eq. (3)	Eq. (4)
^{235}U (10.5)	1.5 ± 0.5	1.5 ± 0.5	0.9 ± 0.6	0.9 ± 0.6	1.4 ± 0.6	1.5 ± 0.6	–	–
^{238}U (12.0)	1.5 ± 0.5	1.5 ± 0.5	0.9 ± 0.6	0.9 ± 0.6	1.4 ± 0.6	1.5 ± 0.5	–	–
^{235}U (18.0)	5.2 ± 0.8	4.8 ± 0.8	5.2 ± 0.9	4.9 ± 0.9	5.1 ± 0.8	4.8 ± 0.8	4.9 ± 1.0	4.6 ± 0.9
^{238}U (18.0)	5.1 ± 0.7	4.7 ± 0.7	5.1 ± 0.8	4.8 ± 0.7	5.0 ± 0.7	4.7 ± 0.7	4.8 ± 0.8	4.5 ± 0.7

$P(A_i)$ is the distribution function of nuclear fragments with the mass number $A_i = A_f + i$ and the charge Z_f; and $\varphi_i(U)$ and $P^{(i)}(J)$ are functions that determine the state distributions in the fission fragment (A_i, Z_f) over the excitation energy and spin. Those distribution functions for various isotopes simultaneously enter the numerator and denominator of expression (2), and the mass numbers $A_i = A_f + i$ are concentrated within a narrow interval. Therefore, the dependences $\varphi_i(U)$ and $P^{(i)}(J)$ were assumed to be identical for various isotopes.

In our calculations, we consider the decay of states with the excitation energies within the same interval $\Delta U = 16$ MeV for all isotopes. The distribution functions of states over the excitation energy, $\varphi_i(U)$, were chosen in the step-like form. Note that the value $\Delta U = 16$ MeV corresponds to the doubled value of the average energy of neutron separation $\bar{S}_n = 8$ MeV (i.e. $\Delta U = 2\bar{S}_n$) and involves almost all excited states that can populate the ground and isomeric states of the researched nucleus (see Figs. 6 and 7). The minimum, $U_0^{(i)}$, and maximum, $U_m^{(i)}$, excitation energies of neutrons occupying the g- and m-states in the nucleus-fragment (A_i, Z_f) were taken equal to $U_0^{(i)} = S_i$ and $U_m^{(i)} = S_i + \Delta U$, respectively. Here, $S_i = \sum_{j=0}^{j=i} S_n^{(j)}$ is the energy needed to separate i neutrons from the nucleus $(A_f + i, Z_f)$, $S_n^{(j)}$ is the separation energy for one neutron, and $S_{i=0} = 0$.

Standard expressions were used for the spin distribution functions of initial states [9, 10]:

$$P^{(i)}(J) = (2J+1)\exp\left(-J(J+1)/2B^2 - \lambda J\right), \quad (3)$$

and

$$P^{(i)}(J) = (2J+1)\exp\left(-J(J+1)/2(B+\mu)^2\right). \quad (4)$$

As was done in Refs. [9, 10], the parameter B in formulas (3) and (4) was calculated in the framework of the Fermi model for the gas of spherical nuclei. The parameters λ and μ were found by fitting the theoretical values of isomeric ratio (2) to experimental data. After the parameters in the spin distribution functions had been determined, the mean angular momentum of the primary fragment (A_f, Z_f) was calculated, by using the formula

$$\bar{J} = \sum_J J\, P^{(0)}(J, x) / \sum_J P^{(0)}(J, x). \quad (5)$$

Summation over the spin J in Eqs. (2) and (5) is carried out over the integer values of $J \geq 0$ for the fission fragments with the integer spin in the ground state and the half-integer values $J \geq 1/2$ for fragments with the half-integer spin in the ground state.

In Figs. 6 and 7, the probabilities of population of the ground and isomeric, respectively, states of ^{97}Nb nucleus from the states (U, J) of excited niobium isotopes with the mass numbers $A_i = \{97, 99\}$ are shown in relative unities. They were calculated with the use of the EMPIRE 3.2 code. The values of those probabilities calculated with the help of the TALYS 1.6 code are similar.

When calculating the populations, various expressions were used for the radiation strength functions and the nuclear level densities [18–20]. The results of calculations for the mean angular momenta, which are similar to the dependences shown in the figures, depend insignificantly on those expressions.

The results of calculations of the mean angular momentum $\bar{J}$ carried out for the primary nucleus of ^{97}Nb fragment are quoted in Table 4. For illustrative purposes, they are also depicted in Fig. 8. From Figs. 6–8, one can see that the emission of different numbers

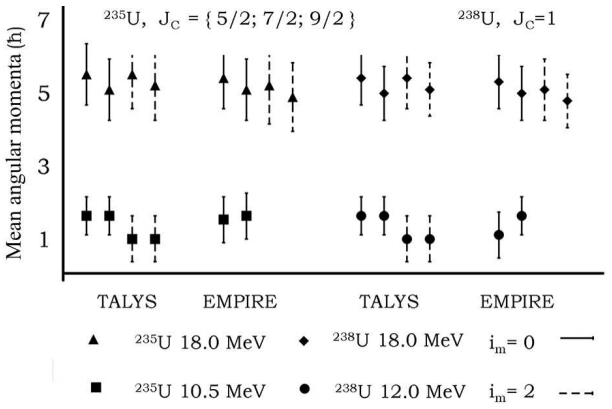

Fig. 8. Results of theoretical calculations for the mean angular momenta taking ($i_m = 2$) and not taking ($i_m = 0$) the neutron emission into account. Calculations were performed with the help of the EMPIRE and TALYS codes. Compound nuclei and their possible spins are indicated

of neutrons gives rise to a certain averaging over the level populations, but this fact does not substantially affects the calculation results for the mean angular momentum. This fact is confirmed by analytical calculations in Ref. [10].

At high excitation energies, the mean angular momenta in the fission fragments differ from the values in the parent nucleus, which testifies that there is a mechanism generating an additional angular momentum. Note that the increase of the isomeric ratios with the end-point energy E_e also gives rise to the increase of the mean angular momenta of primary fission fragments. This relation may probably be associated with the opening of the (γ, nf) reaction channel and may bring about a modification of the distribution for every quantity in Eq. (2).

4. Conclusions

New data have been obtained for the isomeric ratios of ^{97}Nb nucleus that is formed as a result of the photofission of ^{235}U and ^{238}U nuclei by the bremsstrahlung with end-point energies of 10.5, 12.0, and 18.0 MeV. The calculations were carried out with the use of the activation method and with regard for the contribution of the isobaric precursor nucleus to the population. A distinction of the isomeric ratio values obtained at $E_e = 10.5$ and 12 MeV from the values obtained at $E_e = 18$ MeV was demonstrated. This difference may testify that the isomeric ratios considerably depend on the type of the input channel.

The values of mean angular momenta of the fission fragments were determined theoretically with the use of the software codes TALYS 1.6 and EMPIRE 3.2. The possibility for the ^{97}Nb states to be populated after the emission of up to two neutrons owing to the decay of primary fragments with the number of neutrons larger than in ^{97}Nb was taken into consideration. The average angular momenta of primary photofission fragments calculated taking and not taking the emission of neutrons into account coincide within the measurement error. The difference between the values of mean angular momenta for the fission fragments and the corresponding value for the parent nucleus testifies to the presence of an additional mechanism of angular momentum formation.

1. R. Vandenbosh, J.R. Huizenga. *Nuclear Fission* (Academic Press, 1973).
2. D.C. Aumann, W. Guckel, E. Nirschl, H. Zeising. Independent isomeric yield ratio of ^{148}Pm in fission of the moderately excited ^{236}U compound nucleus as a measure of fragment angular momentum. *Phys. Rev.* **16**, 254 (1977) [DOI: 10.1103/PhysRevC.16.254].
3. V.Yu. Denisov, S.V. Reshitko. Mean angular momentum of nuclear-fission fragments. *Phys. At. Nucl.* **62**, 1806 (1999).
4. I.N. Mikhailov, P. Quentin, Ch. Briancon. Angular momentum of fission fragments. *Phys. At. Nucl.* **64**, 1185 (2001).
5. M.G. Davydov, V.G. Magera, A.V. Trukhov. Isomeric yield ratios of photonuclear reactions. *At. Energiya* **62**, 236 (1987) (in Russian).
6. M.G. Davydov, V.G. Magera, A.V. Trukhov, E.M. Shomurodov. Isomeric yield ratios of photonuclear reactions for γ-activation analysis. *At. Energiya* **58**, 47 (1985) (in Russian).
7. I.N. Vishnevskii, V.Yu. Denisov, V.A. Zheltonozhskyi, S.V. Reshit'ko, L.V. Sadovnikov, N.V. Strilchuk. Mean angular momenta of ^{232}Th fission fragments. *Yad. Fiz.* **61**, 1562 (1998) (in Russian).
8. I.N. Vishnevskii, O.I. Davydovskaya, V.A. Zheltonozhskyi, A.N. Savrasov. Research of ^{232}Th and ^{238}U photofission. *Izv. Ross. Akad. Nauk Ser. Fiz.* **73**, 782 (2009) (in Russian).
9. I.M. Vyshnevskyi, V.O. Zheltonozhskii, A.M. Savrasov, E.P. Rovenskykh, V.A. Plujko, O.I. Davydovska, O.M. Gorbachenko. Isomer yield ratios of ^{133}Te, ^{134}I, ^{135}Xe in photofission of ^{235}U with 17 MeV bremsstrahlung. *Yad. Fiz. Energet.* **15**, 111 (2014) (in Ukrainian).
10. I.M. Vyshnevskyi, V.O.Zheltonozhskyi, V.A. Plujko, A.M. Savrasov, O.M. Gorbachenko, O.I. Davydovska, E.P. Rovenskykh. Isomeric yield ratios and mean angular momenta of ^{235}U, ^{237}Np, and ^{239}Pu photofission fragments. *Yad. Fiz. Energet.* **16**, 5 (2015) (in Ukrainian).

11. I.N. Vishnevskii, V.A. Zheltonozhskii, A.N. Savrasov, V.P. Khomenkov, V.A. Plujko, E.P. Rovenskykh. Measurement of isomeric ratios in ^{235}U, ^{237}Np, and ^{239}Pu photofission. *Vopr. At. Nauki Tekhn. Ser. Fiz. Yad. Reakt.* **1**, 79(2015) (in Russian).
12. V.P. Khomenkov. Ph.D. thesis *Investigation of Atomic-Nuclear Effects in the Process of Gamma-Ray Internal Conversion* (Institute for Nuclear Research, Kyiv, 2003) (in Ukrainian).
13. R.B. Firestone, V.S. Shirley, C.M. Baglin. *Table of Isotopes* (Wiley, 1996).
14. H. Naik, G.N. Kim, R. Schwengner, K. Kim, M. Zaman, S.C. Yang, S.G. Shin, Y.-U. Kye, R. Massarczyk, R. John, A. Junghans, A. Wagner, A. Goswami, M.-H. Cho. Measurement of isomeric ratios for ^{89g,m}Zr, ^{91g,m}Mo, and ^{97g,m}Nb in the bremsstrahlung end-point energies of 16 and 45–70 MeV. *Eur. Phys. J. A* **52**, 47 (2016) [DOI: 10.1140/epja/i2016-16047-8].
15. H. Warhalek, R. Vandenbosh. Relative cross-sections for formation of the shielded isomeric pair ^{134m}Cs and ^{134}Cs in medium energy fission. *J. Inorg. Nucl. Chem.* **26**, 669 (1964).
16. M. Herman, R. Capote, B.V. Carlson, P. Obložinský, M. Sin, A. Trkov, H. Wienke, V. Zerkin. EMPIRE: Nuclear reaction model code system for data evaluation. *Nucl. Data Sheets* **108**, 2655 (2007) [DOI: 10.1016/j.nds.2007.11.003]; http://www.nndc.bnl.gov/empire/.
17. A.J. Koning, S. Hilaire, M.C. Duijvestijn. TALYS-1.0. In *Proceedings of the International Conference on Nuclear Data for Science and Technology, 22–27 May, 2007, Nice, France* (EDP Sciences, 2008), p. 211; http://www.talys.eu/.
18. R. Capote, M. Herman, P. Obložinský, P.G. Young, S. Goriely, T. Belgya, A.V. Ignatyuk, A.J. Koning, S. Hilaire, V.A. Plujko, M. Avrigeanu, O. Bersillon, M.B. Chadwick, T. Fukahori, Zhigang Ge, Yinlu Han, S. Kailas, J. Kopecky, V.M. Maslov, G. Reffo, M. Sin, E.Sh. Soukhovitskii, P. Talou. RIPL – Reference input parameter library for calculation of nuclear reactions and nuclear data evaluations. *Nucl. Data Sheets* **110**, 3107 (2009) [DOI: 10.1016/j.nds.2009.10.004]; http://www-nds.iaea.org/RIPL-3/.
19. V.A. Plujko, R. Capote, O.M. Gorbachenko. Giant dipole resonance parameters with uncertainties from photonuclear cross sections. *At. Data Nucl. Data Tabl.* **97**, 567 (2011) [DOI: 10.1016/j.adt.2011.04.001].
20. V.A. Plujko, O.M. Gorbachenko, E.P. Rovenskykh, V.A. Zheltonozhskii. Average description of dipole gamma transitions in hot atomic nuclei. *Nucl. Data Sheets* **118**, 237 (2014) [DOI: 10.1016/j.nds.2014.04.046].

Received 11.07.16.
Translated from Ukrainian by O.I. Voitenko

В.О. Желтоножський, А.М. Саврасов, К.М. Солодовник, В.А. Плюйко, О.М. Горбаченко, О.І. Давидовська

ІЗОМЕРНІ ВІДНОШЕННЯ ТА СЕРЕДНІ КУТОВІ МОМЕНТИ ПЕРВИННИХ ФРАГМЕНТІВ ^{97}Nb ПРИ ФОТОПОДІЛІ ^{235}U ТА ^{238}U

Р е з ю м е

Виміряно ізомерні відношення виходу ^{97}Nb при фотоподілі ядер ^{235}U та ^{238}U гальмівним випромінюванням з граничними енергіями 10,5, 12,0 та 18,0 МеВ. Визначені середні кутові моменти первинних фрагментів фотоподілу за допомогою узагальненої статистичної моделі Хьюзенга–Ванденбоша із використанням кодів TALYS 1.6 та EMPIRE 3.2.